

Performance Analysis of Hybrid 5G Cellular Networks Exploiting mmWave Capabilities in Suburban Areas

Muhammad Shahmeer Omar*, Muhammad Ali Anjum*, Syed Ali Hassan*, Haris Pervaiz[†] and Qiang Ni[†]

*School of Electrical Engineering & Computer Science (SEECs),
National University of Sciences & Technology (NUST), Islamabad, Pakistan
{11beemomar, 11besemanjum, ali.hassan}@seecs.edu.pk

[†]School of Computing & Communications, Lancaster University, UK
{h.pervaiz, q.ni}@lancaster.ac.uk

Abstract—Millimeter wave (mmWave) technology is considered as a key enabler for fifth generation (5G) networks to achieve higher data rates with low transmission power by offloading the users with low signal-to-noise-ratios. Millimeter wave networks operating at E and W frequency bands have available bandwidth of 1 GHz or more to provide higher data rates whereas their propagation characteristics differ greatly from the conventional Ultra High Frequency (UHF) networks operating at sub 6 GHz frequency band. The purpose of this paper is to investigate the performance in terms of coverage and rate, of hybrid cellular networks where base stations (BSs) operating at mmWave and sub-6 GHz bands coexist in a suburban environment such as a large university campus. Actual building locations are used to model blockages in the said environment. Our analysis highlights the noise limited nature of mmWave networks. Extensive simulation results show the effectiveness of dense mmWave BS deployment to achieve improved coverage and rate probabilities in comparison to the stand alone UHF network.

Index Terms—Millimeter wave, sub 6 GHz band, hybrid networks, 5G networks, Cooperative networks.

I. INTRODUCTION

One of the emerging technologies towards enabling fifth generation (5G) is multiple radio access technologies (multi-RAT) operating at different frequency bands deployed within the same geographical area. The deployment of mmWave BSs has great potential to improve the spatial reuse of radio resources and also to enhance the energy and spectral efficiency of the network. The widespread use of smart phones has resulted in significant increases in data traffic as mentioned in [1]. This traffic surge and the projected traffic requirements combined with congestion in the available spectrum has made evident the need to shift to unused frequency bands. The use of the mmWave band, ranging from 10 GHz to 300 GHz, is an attractive solution to the spectrum congestion problem. Investigation of the use of mmWave technology in 5G cellular networks is already underway [2]– [3].

In the past, mmWave technology was not considered to be feasible for wireless communication due to the larger penetration loss. In [4]– [5], authors have analysed mmWave for cellular networks by using highly directional antennas and beamforming to provide coverage in the range of about 150-200 m. Combining this with the low manufacturing cost of mmWave chips, the deployment of mmWave networks becomes an attractive proposition [6]. In the current state of

the art literature, (such as [7]– [11]), the authors have analysed coverage and rate trends in mmWave cellular networks. The authors in [7] have shown that the mmWave cellular networks are noise limited whereas the conventional UHF cellular networks are interference limited. Recently, a lot of attention has been focussed to analytically model the blockages for urban and dense urban areas as mentioned in [7]– [8] by using the curve fitting techniques, however, these techniques lack the flexibility to be used for suburban areas.

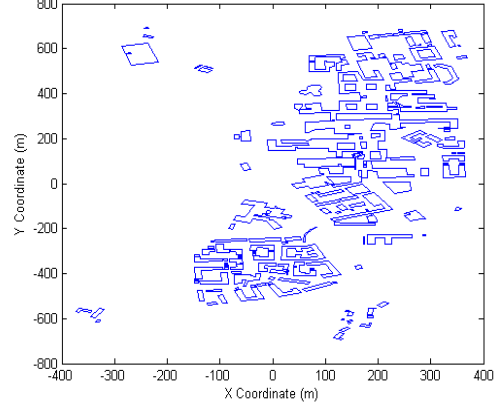
In [9], a line-of-sight (LoS) ball approximation was derived to model the blockages but it was not validated in comparison to the actual blockage scenarios. According to the best of our knowledge, there is very limited work to study the coverage and rate trends of hybrid cellular networks in suburban areas by deriving an approach using the actual building locations to model the blockages. Since buildings are the main source of blockage in the outdoor environments, we have used actual building locations at the Lancaster University (LU) campus to study the rate and coverage trends by varying the proportion of BSs operating in either mmWave or UHF frequency band for different user densities. In this work, we investigate the performance of hybrid cellular network case in addition to conventional UHF and mmWave cellular network only cases.

II. SYSTEM MODEL

We consider the downlink transmission scheme of a hybrid cellular network in which BSs operating in UHF and mmWave frequency bands coexist. In this work, we use the actual building locations from the LU campus as shown in Fig. 1. This incorporates real blockage effects and environmental geometry into our analysis. Fig. 1(a) shows the Google Earth view of the LU campus whereas Fig. 1(b) shows the actual building locations of the campus, extracted using Matlab. Firstly, the shape file covering the $100 \times 100 \text{ km}^2$ area of the relative UK National Grid Reference for Lancaster and its surrounding areas is obtained from [12]. By using the Quantum Geographic Information System (QGIS) software [13], the initial shape file is processed into a smaller shape file consisting of only the region of interest (RoI), i.e., the LU campus. The detailed steps and procedures to achieve the actual building locations have been omitted for brevity. Some of the key building statistics



(a) Google Earth view of Lancaster University



(b) The extracted building locations.

Fig. 1: Considered Region of Interest

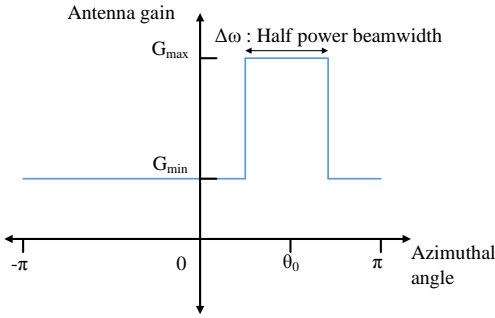


Fig. 2: Antenna Sectoring

of the LU campus, obtained by using our script, are given in Table I.

The mmWave and UHF BSs are uniformly distributed within the RoI, i.e., 1.6 km x 0.8 km rectangular region centered at the origin. The number of users and BSs deployed in this area are modelled by independent Poisson point processes (PPPs) with densities u users/km² and v BSs/km², respectively. We have considered only the outdoor users in this study and the location of each user is averaged over the entire region of interest.

Although, the users are distributed solely in the outdoor regions, BSs may lie within a building, however, for simplicity and without the loss of generality, we assume that such BSs lie on the building rooftops. A communication link is assumed to be non-line-of-sight (NLoS) if the line segment joining the BS and the user is blocked by a building. Otherwise, it is considered to be line-of-sight (LoS). It is also worthwhile to mention that the path loss configurations are different for LoS and NLoS links. The bandwidth allotted to each user depends on the type of communication link, i.e., mmWave or UHF.

TABLE I: Building Statistics for the Region of Interest

% area covered by buildings	Avg. building area (m ²)	Avg. building perimeter (m)
12.63	991.9254	131.8574

A. User Association Metric

For the purpose of this study, *user association* is defined as the process by which a user decides which BS it connects to in the network. The users lying within the considered area are associated with the network offering the highest received signal strength or signal-to-noise-ratio (SNR). The remaining BSs operating in the same frequency band in the network configuration act as interferers. We assume open access, which means a user is allowed to access any BSs operating at either UHF (uhf) or mmWave (mm) frequency band. It is further assumed that the users are associated to a particular BS j given as follows:

$$j = \arg \max_{k \in \{\text{uhf}, \text{mm}\}} P_k \beta_k L_k^{-1}, \quad (1)$$

where P_k is the transmission power of the k^{th} type BS, β_k is the association or bias factor for the k^{th} type BS and L_k^{-1} is the path loss of the user at a distance ‘ r ’ from the k^{th} type BS. If $\beta_k = 1$, then the user association is based on the maximum received power and otherwise the user association is based on the maximum biased received power. In this work, we assume $\beta_{\text{uhf}} = 0$ dB and β_{mm} can have a value between 0 and 10 dB.

In the case of hybrid cellular networks, the BSs operating at UHF and mmWave frequency bands coexist simultaneously. A user $u \in U$ can lie in the following three disjoint sets:

$$u = \begin{cases} U_1 & \text{if } j = \text{uhf}, P_{\text{uhf}} L_{\text{uhf}}^{-1} > P_{\text{mm}} \beta_{\text{mm}} L_{\text{mm}}^{-1}, \\ U_2 & \text{if } j = \text{mm}, P_{\text{mm}} \beta_{\text{mm}} L_{\text{mm}}^{-1} > P_{\text{uhf}} L_{\text{uhf}}^{-1}, \\ U_3 & \text{if } j = \text{mm}, P_{\text{mm}} L_{\text{mm}}^{-1} \leq P_{\text{uhf}} L_{\text{uhf}}^{-1} \leq P_{\text{mm}} \beta_{\text{mm}} L_{\text{mm}}^{-1} \end{cases} \quad (2)$$

In this equation, $U_1 \cup U_2 \cup U_3 = U$. The set U_1 is the set

of users associated with UHF BSs. The set U_2 is the set of unbiased users associated with mmWave BSs and the users offloaded from UHF BSs to the mmWave BSs due to cell range expansion caused by the biasing factor β_{mm} constitute the set U_3 .

III. CHANNEL MODEL

The path loss for mmWave link $L_{\text{mm}}(r)$, in dB, is modeled as

$$L_{\text{mm}}(r) = \begin{cases} \rho + 10\alpha_L \log(r) + \chi_L & \text{if link is LoS} \\ \rho + 10\alpha_N \log(r) + \chi_N & \text{otherwise,} \end{cases} \quad (3a)$$

whereas the path loss for the UHF link, $L_{\text{UHF}}(r)$, in dB, is given by

$$L_{\text{UHF}}(r) = 20\log\left(\frac{4\pi}{\lambda_c}\right) + 10\alpha \log(r) + \chi_{\text{UHF}}, \quad (3b)$$

In the above equations, χ_L and χ_N are the zero mean log normal random variables for LoS and NLoS mmWave links respectively, which model the effects of shadow fading. The fixed path loss in L_{mm} is given by $\rho = 32.4 + 20\log(f_c)$ where f_c is the carrier frequency and λ_c is the wavelength corresponding to the carrier frequency f_c . The symbol χ_{UHF} represents the shadow fading in UHF links. The path loss exponents for LoS and NLoS mmWave links are denoted by α_L and α_N respectively. The path loss exponent for a microwave link is denoted by α and assumed to be 3, unless otherwise stated.

The received power of the user from the mmWave BS at a distance r [m] in the downlink transmission scheme is given as follow:

$$P_{r, \text{mmWave}} = \frac{P_t G(\theta) \mu}{L_{\text{mm}}(r)}. \quad (4a)$$

Similarly, the received power of the user from the UHF BS at a distance r [m] in downlink transmission scheme is given as follow:

$$P_{r, \text{UHF}} = \frac{P_t \mu}{L_{\text{UHF}}(r)}, \quad (4b)$$

where P_t is the transmit power, $L_{\text{mm}}(r)$ and $L_{\text{UHF}}(r)$ are the path losses of mmWave and UHF links, respectively. The symbol θ represents the azimuthal angle of the BS beam alignment and $G(\cdot)$ is the antenna gain as a function of this azimuthal angle. Variation in gain due to elevation angle is ignored in this work. User antennas are assumed to be omnidirectional. The symbol μ represents the squared envelope of the multi-path fading where the envelope follows a Rayleigh or Rician distribution depending on whether the user-BS link is LoS or NLoS, respectively. Both the mmWave and microwave BSs are assumed to have multiple transmitting antennas. In this work, we assume three transmitting antennas per BS. Users are assumed to have a single receiving antenna resulting in a 3 x 1 multiple-input single-output (MISO) system. The angle θ is measured with respect to the beam alignment that provides the maximum received signal power at θ_0 . For a LoS link, θ_0 is the angle of the user with respect to the BS but for an NLoS link, this may be some other angle depending on the geography of

the region. In this work, we assume a sectored approximation to the beam pattern, as shown in Fig. 2. The transmitter beam is said to be perfectly aligned if $\theta \in [\theta_0 - \frac{\Delta\omega}{2}, \theta_0 + \frac{\Delta\omega}{2}]$ where $\Delta\omega$ is the half power beamwidth. A perfectly aligned transmitter beam has a gain of G_{max} but a misaligned beam has gain G_{min} . We assume perfect alignment for the user-BS link under consideration while the interfering link alignments depend on the actual locations of the remaining BSs. Our antenna sectoring model follows the model adopted by the authors in [10].

It is assumed that the users connected to a BS are multiplexed using a time division multiplexing multiple access (TDMA) scheme, so that the thermal noise is collected over the entire system bandwidth. The user is assumed to be at the origin and the paired BS at a distance r , the signal-to-interference plus noise ratio (SINR) of the user is given as follow:

$$\text{SINR} = \begin{cases} \frac{P_{r, \text{mmWave}}}{\sum_{x \in \psi, x \neq r} P_r(x) + \sigma^2} & \text{for mmWave,} \\ \frac{P_{r, \text{UHF}}}{\sum_{x \in \phi, x \neq r} P_r(x) + \sigma^2} & \text{for UHF,} \end{cases} \quad (5)$$

where the noise power (in dB) is calculated as $\sigma^2 = -174\text{dBm/Hz} + 10\log(\text{BHz}) + NF(\text{dB})$ and NF is the noise figure in dB. The SINR coverage probability with a given SINR threshold τ_s is defined as

$$P_C(\tau_s) = \mathbb{P}(\text{SINR} > \tau_s) \quad (6)$$

The downlink rate for a user connected to a BS serving the total number of users N is given by

$$\text{Rate} = \frac{B}{N} \log_2(1 + \text{SINR}) \quad (7)$$

The rate coverage probability for a given rate threshold τ_r is given by

$$P_R(\tau_r) = \mathbb{P}(\text{Rate} > \tau_r) = \mathbb{P}\left(\text{SINR} > 2^{\frac{\tau_r \times N}{B}} - 1\right) \quad (8)$$

IV. PERFORMANCE ANALYSIS

We assume three different network configurations, namely, the stand alone UHF cellular network, stand alone mmWave cellular network and hybrid cellular network. The hybrid network consists of both UHF and mmWave BSs, which are deployed using independent PPPs, denoted by ϕ and ψ with densities v_1 and v_2 , respectively. In this study, we assume that $v_2 = \gamma v_1$, where $\gamma > 1$ implying that the mmWave BS density is greater than the UHF BS density. User densities are denoted by u . The simulation parameters used in our analysis, unless otherwise stated, are given in Table II.

Firstly, we analyse the complimentary cumulative distribution function (CCDF) of the SINR and SNR for both stand alone UHF and mmWave networks, as depicted in Fig. 3. We can observe that there is a minor difference between the coverage probability plots for the SNR and SINR cases in the mmWave network. However, in UHF networks, we can notice that the SNR coverage probability is considerably higher than

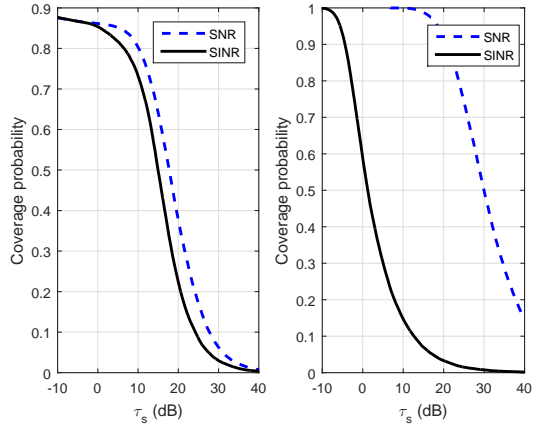


Fig. 3: Comparison of SNR and SINR in mmWave (left) and UHF (right) networks with $v_1 = v_2 = 15$ BSs/km².

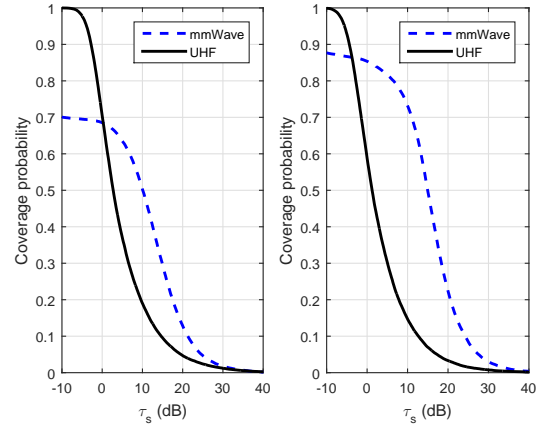


Fig. 4: Comparison of SINR coverage in UHF and mmWave network for $v_1 = v_2 = 5$ BSs/km² (left) and $v_1 = v_2 = 15$ BSs/km² (right).

TABLE II: Simulation Parameters

Parameter	Value	Parameter	Value
$f_{c,mm}$	73 GHz	Bw_{mm}	2 GHz
$f_{c,UHF}$	2.4 GHz	Bw_{UHF}	20 MHz
P_t	30dBm	NF	10 dB
u	200 users/km ²	$\Delta\omega$	10°
α_L	2	α_N	3.3
$Std(\chi_L)$	5.2 dB	$Std(\chi_N)$	7.2 dB
$Std(\chi)$	4 dB	Rician K-factor	4 dB

the SINR coverage probability, highlighting the interference limited nature of UHF networks. On the other hand mmWave networks are noise limited due to the negligible impact of interference and the greater available bandwidth in mmWave networks operating at the 73 GHz frequency band.

Fig. 4 compares the SINR coverage probability of the mmWave and UHF networks at two different BS densities. We can observe that the UHF network exhibits greater coverage probabilities at lower SINR thresholds as UHF networks provide greater SINR at the cell edge whereas the mmWave network offers better coverage to the users located close to the BSs due to low interference from the neighbouring mmWave BSs. Increasing BS density can lead to an improvement in SINR coverage probability for the mmWave networks as the average distance between the user and BS can be reduced in this scenario. For example, at a given SINR threshold of 10 dB, the coverage probability is improved from 0.5 to 0.7 as the mmWave BS density is increased from 5 BSs/km² to 15 BSs/km². Hence, the figure reveals that stand alone mmWave network needs to be deployed with the greater BS densities in comparison to the stand alone UHF network.

Rate coverage probabilities of UHF and mmWave networks for different user densities are shown in Fig. 5. We can observe from the figure that the mmWave network can provide high

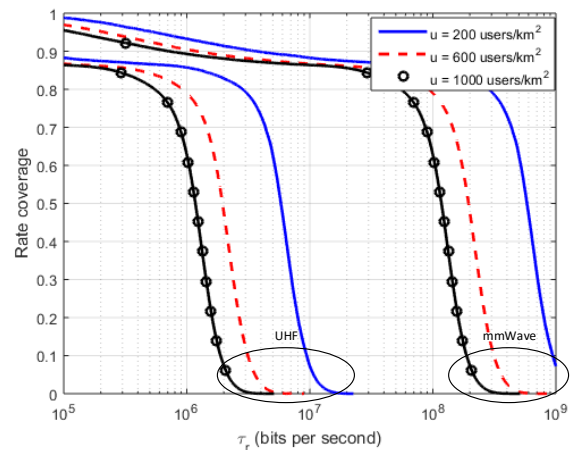


Fig. 5: Rate coverage for mmWave and UHF networks for different user densities with $v_1 = v_2 = 15$ BSs/km².

data rates in comparison to the UHF network. Approximately 80% of users in the UHF network experience rates of up to 3 Mega bits per second (Mbps) whereas in the mmWave network the same proportion of users experience rates of up to 300 Mbps at a user density of 200 users/km². The figure also reveals that an increase in user density decreases the achievable data rates due to an increase in the number of users associated with each BS.

Fig. 6 shows the rate coverage probability of the mmWave network for different BS densities. It shows that greater the BS density, the better the rate coverage of the network, for example, for $\tau_r = 10$ Mbps a mmWave network with BS densities of 5, 10, 15 BSs/km² show rate coverage probabilities of 68%, 82% and 89%, respectively. This is because a larger number of BSs lowers the number of users connected to each individual BS resulting in higher available bandwidth. The rate coverage probability for the lower rate thresholds, which represents the data rates of cell edge users, also increases with

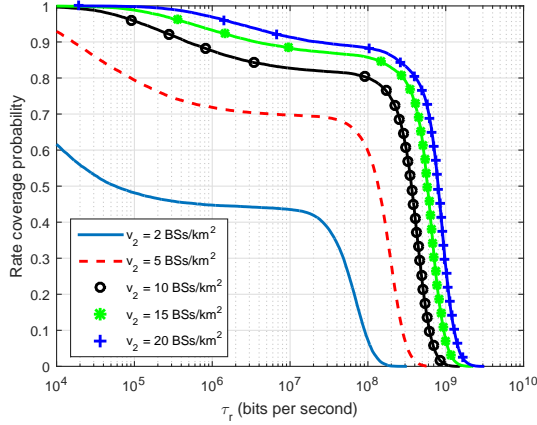


Fig. 6: Rate coverage probability of mmWave networks for different BS densities.

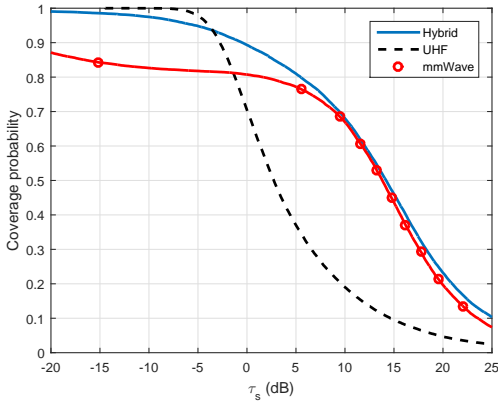


Fig. 7: SINR coverage probability for hybrid networks ($v_1 = 5$ BSs/km², $v_2 = 10$ BSs/km²) and stand alone networks.

an increase in BS density. We can also observe that an increase in rate coverage is diminishing for larger BS densities alluding to the fact that there is an optimal BS density when considering total system power and the rate coverage.

We plot the SINR coverage probability versus different SINR thresholds for hybrid and standalone networks in Fig. 7. At lower SINR thresholds, the hybrid network offers better SINR coverage probability than mmWave networks but marginally worse than that of a stand alone UHF network. At SINR thresholds greater than -5 dB, the hybrid network shows an improvement in SINR coverage probability over UHF networks. The stand alone mmWave and hybrid network SINR trends begin to converge at greater thresholds. The greater path loss associated with mmWave severely restricts its ability to form links over long distances, which is apparent in the results in Fig. 4. Greater transmission range of UHF BSs improves reception for users located at the cell edge. This combined with the high directional antenna gain due to beamforming alignment in the mmWave network significantly improves SINR coverage in the hybrid network. It is pertinent

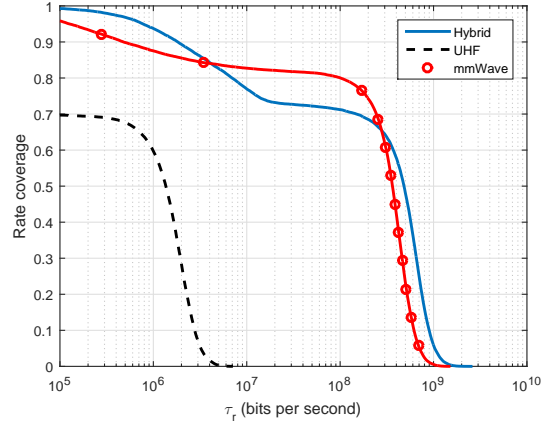


Fig. 8: Rate coverage probability for hybrid networks ($v_1 = 5$ BSs/km², $v_2 = 10$ BSs/km²) and stand alone networks.

to note that the hybrid network has a total BS density of 15 BSs/km² where $v_1 = 5$ BSs/km² and $v_2 = 10$ BSs/km². The BS densities of the stand alone UHF and mmWave networks are denoted by v_1 and v_2 , respectively.

Fig. 8 compares the rate coverage probability of the hybrid network to those of the stand alone mmWave and UHF networks. The network setup is the same as the one used in Fig. 7. From the figure, we can observe that the rate coverage probability of the hybrid network is similar to that of the mmWave network at lower rate thresholds. The hybrid network rates fall off from the stand alone mmWave network rates which occurs due to the presence of UHF links. Since users can have both kinds of links in the hybrid network, the probability of achieving data rates as large as a stand alone mmWave network is lowered. For a rate coverage probability of 70%, the stand alone mmWave network allows data rates upto 400 Mbps, the hybrid network allows rates of upto 100 Mbps and the UHF network allows rates of upto 100 Kilo bits per second (Kbps). Hence, it can be seen from the results in Fig. 7 and Fig. 8 that using a hybrid network bolsters reception quality of mmWave signals but at the cost of data rates.

Fig. 9 shows a comparison of the different network

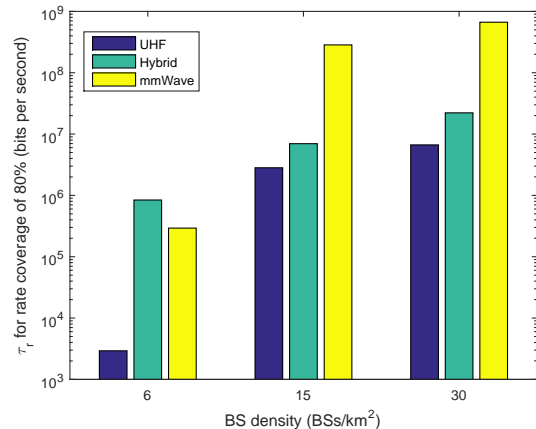


Fig. 9: Data rates for different network topologies at a fixed rate coverage of 0.8.

topologies in terms of the rates allowed for each network for rate coverage probability of 80%. In this simulation setup, the hybrid network is setup such that $v_2 = 2v_1$. In this simulation setup, the total BS density of the stand alone and hybrid networks is same. When total BS density is 6 BSs/km² the hybrid network offers the greatest rates. This is due to the fact that the stand alone UHF network has less available bandwidth restricting its achievable data rates and the lower SINR coverage probability of the mmWave network at lower BS densities. As the total BS density is increased, the rates for all three networks also improves. The mmWave network rates overtake those offered by the hybrid network at greater BS densities. For example, the hybrid network provide a data rate of 6 Mbps to 80% of the users at a BS density of 15 BSs/km². However, the mmWave network provide data rate of 280 Mbps at the BS density of 15 BSs/km² for the rate coverage probability of 80%. From the figure, we can also observe a diminishing increase in rate as BS density is increased.

Fig. 10 shows the proportion of the users associated to the mmWave BSs for the varying biasing factor β_{mm} of the hybrid cellular network for different values of ϵ . ϵ is the ratio of BSs operating at mmWave frequency band of 73 GHz to the total number of BSs and is defined as $\epsilon = \frac{v_2}{v_1 + v_2}$. The figure reveals the impact of varying β_{mm} and the UHF path loss exponent α on the user association metric according to the *user association policy* defined in (1). As the β_{mm} is increased from 0 to 10 dB, for a given mmWave and UHF BSs densities, the proportion of users associated with mmWave BSs also increases, which is clearly evident from the figure. By increasing (or decreasing) the density of mmWave (or UHF) BSs reduces the average distance of the user from the mmWave BS resulting in an improved received power. The figure also highlights the impact of UHF path loss exponent on the user association metric. An increase in the path loss exponent of UHF results in an increase in the proportion of users associated

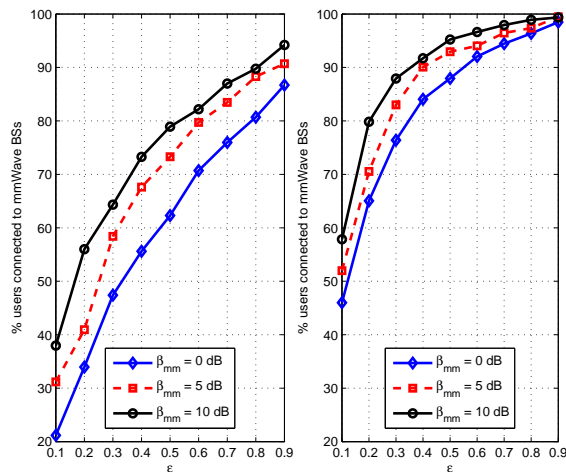


Fig. 10: User association for different values of ϵ with $v_1 + v_2 = 20$ BSs/km² for $\alpha = 3$ (left) and $\alpha = 4$ (right).

with mmWave BSs due to the less biased received power to the user from UHF BSs.

V. CONCLUSION

In this paper, we have investigated the coverage and rate trends in a downlink transmission scheme of hybrid cellular networks for different proportions of UHF and mmWave BSs with varying user densities. We have also investigated the impact of different factors, such as the UHF path loss exponent and biasing factor, on user association in a hybrid network while incorporating realistic outdoor blockage effects in a suburban environment. Simulation results show that the hybrid cellular networks achieve a rate coverage comparable to that of the stand alone mmWave network and much higher than that of the stand alone UHF network. We observe that the hybrid network offers better SINR coverage than the stand alone mmWave network, especially when considering SINR coverage at the cell edge. The investigation may be extended to include the energy efficiency of hybrid networks, while implementing different user association schemes, and to study their impact on network performance in the future.

REFERENCES

- [1] Cisco, "Cisco Visual Networking Index: Global Mobile Data Traffic Forecast Update, 2012-2017," Whitepaper, available at: <http://goo.gl/xxLT>.
- [2] T. S. Rappaport, R. W. Heath Jr., R. C. Daniels, J. N. Murdock, *Millimeter Wave Wireless Communication*, Prentice Hall, 2014.
- [3] T. S. Rappaport, S. Sun, R. Mayzus, H. Zhao, Y. Azar, K. Wang, G. N. Wong, J. K. Schulz, M. Samimi, F. Gutierrez, "Millimeter Wave Mobile Communications for 5G Cellular: It Will Work!," in *IEEE Access*, vol.1, pp.335-349, May 2013.
- [4] Y. Azar, G. N. Wong, K. Wang, R. Mayzus, J. K. Schulz, H. Zhao, F. Gutierrez, D. Hwang, T. S. Rappaport "28 GHz propagation measurements for outdoor cellular communications using steerable beam antennas in New York City," *IEEE ICC*, pp. 5143-5147, Jun. 2013.
- [5] T. S. Rappaport, E. Ben-Dor, J. N. Murdock, Yijun Qiao, "38 GHz and 60 GHz angle-dependent propagation for cellular and peer-to-peer wireless communications," *IEEE ICC*, pp. 4568-4573, Jun. 2012.
- [6] T. Rappaport, J. N. Murdock, F. Gutierrez, "State of art in 60 GHz integrated circuits and systems for wireless communication," *Proc. IEEE*, vol. 99, no. 8, pp. 1390-1436, Aug. 2011.
- [7] S. Rangan, T. S. Rappaport, E. Erkip, "Millimeter wave cellular wireless networks: Potentials and challenges," *Proc. IEEE*, vol. 102, no. 3, pp. 366-385, Mar. 2014.
- [8] A. Ghosh, T. A. Thomas, M. C. Cudak, R. Ratasuk, P. Moorut, F. W. Vook, T. S. Rappaport, G. R. MacCartney, S. Sun, S. Nie, "Millimeter wave enhanced local area systems: A high data rate approach for future wireless networks," *IEEE J. Sel. Areas Commun.*, vol. 32, no. 6, pp. 1152-1163, Jun. 2014.
- [9] T. Bai, R. W. Heath, "Coverage and Rate Analysis for Millimeter-Wave Cellular Networks," in *IEEE Trans. on Wireless Comm.*, vol. 14, no. 2, pp.1100-1114, Feb. 2015.
- [10] M. N. Kulkarni, S. Singh, J. G. Andrews, "Coverage and rate trends in dense urban mmWave cellular networks," in *2014 IEEE Global Communications Conference (GLOBECOM)*, pp.3809-3814, Dec. 2014.
- [11] S. Singh, M. N. Kulkarni, A. Ghosh, J. G. Andrews, "Tractable model for rate in self-backhauled millimeter wave cellular networks," in *IEEE J. Sel. Areas Commun.*, vol.33, no.10, pp.2196-2211, Oct. 2015.
- [12] Ordinance Survey (OS) OpenData. [Online]. Available: <https://www.ordnancesurvey.co.uk/opendatadownload/products.html>.
- [13] QGIS: A free and open source geographic information system. [Online]. Available: <http://www.qgis.org/en/site/>.